Title

Sympathetic nervous system hyperactivity results in potent cerebral hypoperfusion in swine.

Authors

Kim, Wi Jin
Dacey, Michael
Samarage, Hashitha Milan
et al.

Publication Date

2022-09-01

DOI

10.1016/j.autneu.2022.102987

Peer reviewed

HHS Public Access

Author manuscript

Auton Neurosci. Author manuscript; available in PMC 2022 November 13.

Published in final edited form as:

Auton Neurosci. 2022 September ; 241: 102987. doi:10.1016/j.autneu.2022.102987.

Sympathetic nervous system hyperactivity results in potent cerebral hypoperfusion in swine

Wi Jin Kim, MD[1,*], **Michael Dacey, MD PhD**[2,*], **Hashitha Milan Samarage, MBBS**[1], **David Zarrin, BS**[3], **Keshav Goel, BS**[3], **Christopher Chan, BS**[2], **Xin Qi, BS**[3], **Anthony Wang, MD**[1], **Kalyanam Shivkumar, MD PhD**[2], **Jeffrey Ardell, PhD**[2], **Geoffrey Colby, MD PhD**[1]

[1]Department of Neurosurgery, University of California Los Angeles, Los Angeles, California, USA

[2]Department of Cardiac Arrhythmia Center, University of California Los Angeles, Los Angeles, California, USA

[3]David Geffen School of Medicine, University of California Los Angeles, Los Angeles, California, USA

Introduction

To ensure adequate brain perfusion, cerebral blood flow is tightly regulated through myogenic, neurogenic, metabolic and endothelial processes known as autoregulation.[1] Cerebral vasospasm is a complex disease process involving multiple mechanisms that results in reversible narrowing of blood vessels, often leading to permanent stroke and poor patient outcomes.[2] It occurs in up to 50–90% of patients with aneurysmal subarachnoid hemorrhage, and 60% of patients with traumatic brain injury, making it one of the leading causes of preventable morbidity in these patients.[3,4] Yet, there are limited durable treatment modalities for patients experiencing cerebral vasospasm; intra-arterial calcium channel blockers are moderately effective but short-acting, and balloon angioplasty has limited access to distal vessels with higher risks of vessel dissection and rupture. Hence, targeted therapies to augment cerebral blood flow in disease states of cerebral hypoperfusion, such as cerebral vasospasm, are of immediate clinical importance.

One of the key mechanisms underlying vasospasm is likely sympathetically-mediated vasoconstriction.[5–8] Cerebral arteries are innervated by the autonomic nervous system; vasoconstriction and vasodilation are mediated by sympathetic and parasympathetic activation, respectively.[9–12] Numerous studies have shown increased catecholamine release in patients with non-traumatic subarachnoid hemorrhage and cerebral vasospasm, consistent with increased sympathetic activation.[5,6,8] Intracranial sympathetic perivascular nerve fibers have been found to primarily originate from the ipsilateral superior cervical ganglion

Corresponding Author: Geoffrey P. Colby MD, PhD, MAANS, UCLA Neurosurgery, 300 Stein Plaza 420, Los Angeles, California 90095, Telephone: 310-794-7108, gcolby@mednet.ucla.edu.

*These authors contributed equally to this work

Previous Presentations: None

Financial Disclosures: Casa Colina Foundation research grant, NIH Research Education Programs (R25)

Conflicts of Interest: None

(SCG).[13–15] Inhibition of SCG suppressed intracerebral vasoconstriction in rat models with subarachnoid hemorrhage or global cerebral ischemia.[16,17] In fact, a regional percutaneous anesthetic block to the cervical sympathetic ganglion in a small clinical study involving nine patients with vasospasm after aneurysmal subarachnoid hemorrhage was shown to improve cerebral perfusion.[18]

There is a need to better understand and define the role of sympathetic-mediated vasospasm, but to date, a robust animal model does not exist, limiting mechanistic understanding and therapeutic development. Our study aims to further elucidate the role of SCG in modulating the sympathetic tone of cerebral vasculature and to demonstrate that its hyperactivity can result in significant cerebral hypoperfusion in large mammals. We also demonstrate that direct inhibition of the superior cervical ganglion with local anesthetic is able to inhibit its effects and restore normal cerebral perfusion.

Methods

Animal Care

Use of animals, associated housing/handling and all related experiments were reviewed and approved by the institution's Institutional Animal Care and Use Committee and Animal Research Committee and Division of Laboratory Animal Medicine. All procedure was done in accordance with the Association for Assessment and Accreditation of Laboratory Animal Care International guidelines.

Anesthesia

Yorkshire pigs (Sus scrofa) of either gender between 40–50kg were used. Animals were pre-sedated with intramuscular Telazol and transitioned to inhaled isoflurane for intubation and intravenous (IV) access. General anesthesia was maintained with inhaled isoflurane during the surgical preparation and transitioned to α-chloralose upon completion of the neck dissection to minimize blunting of the autonomic reflexes by isoflurane. A-chloralose was prepared and administered as previously described.[19] All computed tomography images were obtained at least 30 minutes after completely weaning off of the isoflurane. Vitals were continuously measured and recorded every five minutes. All animals were ventilated with 2L of supplemental oxygen, with tidal volume of 400mL and respiratory rate of 12 per minute.

Neck Dissection

After standard preparation of the surgical field, high anterolateral cervical incisions were made bilaterally along the medial border of the sternocleidomastoid muscles and dissection was carried down to the carotid sheath in a typical carotid endarterectomy approach. Contents of the carotid sheath were identified (Figure 1), while preserving the anatomical integrity of the sympathetic trunk in close proximity to the carotid artery. The SCG was reliably identified near the branch point of the ascending pharyngeal artery.

SCG Stimulation

Bipolar needles (platinum iridium) were inserted into the identified SCG and was stimulated electrically using a Grass Stimulator. Square wave stimulation began at 1mA and increased

in 0.5mA increments until ipsilateral mydriasis was noted with fixed supramaximal frequency (10Hz) and pulse-width (4ms). SCG was stimulated at twice the magnitude of current required to induce ipsilateral mydriasis to ensure adequate stimulation. Computed tomography perfusion (CTp) scans were obtained at least 30 seconds after the onset of SCG stimulation. SCG stimulation was discontinued after completion of the CT scan, and a minimum of 15 minutes were allotted to ensure all effects of the stimulation had returned to baseline physiologic state, prior to further testing.

CTp Scan

Images were obtained using a 2012 Siemens SOMATOM Definition AS Computed Tomography scanner (Spatial resolution: 30lp/cm. Temporal resolution: 150ms). Each scan had an acquisition time of 38.63 seconds, consisting of 25 passes with 1.50 seconds per pass. These parameters were selected to fully capture the contrast bolus passing through the cerebral vasculature. Bayer HealthCare MEDRAD Stellant contrast injector was used to deliver 50mL of Omnipaque (iohexol) 300 into the ear vein at a rate of 5mL/s with a pressure limit of 325psi. Imaging acquisition was started before the contrast bolus to capture peak and trough contrast enhancement throughout the study.

Lidocaine Injection to SCG

A 29G needle was used to deliver 0.3mL of 2% Lidocaine HCL to the identified SCG. Electrical stimulation of the SCG was initiated at least 90 seconds after the lidocaine injection to ensure adequate time for the lidocaine to take effect.

Image Processing and Analysis

CTp data were analyzed with the commercially available and clinically utilized software, Syngo.via (Siemens Healthcare, Germany). Each scan was evaluated using time-enhancement curves with user-selected references for arterial and venous phases at the common carotid artery and superior sagittal sinus, respectively. Algorithm inherent to the software was used to determine cerebral blood flow (CBF), cerebral blood volume (CBV), mean transit time (MTT) and time-to-maximum (TMax). Regions of interest (ROI) were selected on the right hemisphere at frontal, temporal, parieto-occipital and posterior-fossa regions (Figure 2). A duplicate corresponding ROI was automatically generated on the left side by the software, by mirroring the right ROI across the mid-sagittal plane (Figure 3). Mean values for each ROI were calculated and used for subsequent analyses.

Statistics

To account for variability between animals and between scans, ROIs described above were analyzed in relation to the laterality of the stimulus (i.e., ipsilateral SCG stimulated ROI as a percentage of contralateral non-SCG stimulated ROI). The percent difference of each ROI compared to contralateral unaffected side was determined. Two-tailed student’s t-test was used to compare the generated means of the difference with or without SCG stimulation to determine statistical significance between different parameters. The significant level for all tests was set at $p=0.05$.

Results

Seventeen Yorkshire swine were used for the study. Two animals were excluded due to difficulty identifying the SCG and failure to elicit ipsilateral pupillary dilation with electrical stimulation. Mean weight of animals was 43.2 ± 2.95kg; mean temperature was 100.3 ± 0.88°F; mean heart rate was 88 ± 15bpm; mean oxygen saturation was 97.3 ± 3.85%; mean systolic blood pressure was 112 ± 21.9mmHg; mean diastolic blood pressure was 71.0 ± 21.1mmHg; mean mean arterial pressure was 80.0 ± 28.6mmHg; mean end tidal carbon dioxide was 41.5 ± 2.39mmHg. There were no significant changes to temperature or hemodynamic parameters during SCG stimulation to indicate a systemic sympathetic response. CTp data at baseline and with SCG stimulation was obtained for 29 SCGs (15 left and 14 right stimulations). CTp for SCG blockade with stimulation was obtained for 14 SCGs (8 left and 6 right stimulations).

SCG stimulation causes ipsilateral cerebral perfusion deficit

At baseline, there was no difference in CBF, CBV, MTT and TMax between the right and left side in the frontal, temporal parieto-occipital and posterior-fossa regions of interest as measured by CTp. Stimulation of the SCG caused ipsilateral global reduction in CBF as measured by CTp in all ROI (Figure 3).

There was an approximate 20–30% reduction in ipsilateral CBF with SCG stimulation compared to the contralateral non-stimulated side (Figure 4). Mean CBF decreased by 27.4% and 26.3% in frontal regions, 30.8% and 30.4% in temporal regions, 30.8% and 30.3% in parieto-occipital regions, and 23.0% and 19.0% in posterior-fossa regions with right and left side SCG stimulations respectively, compared to non-stimulated contralateral side (all p-values < 0.001).

CBV also decreased by approximately 10–25% with ipsilateral SCG stimulation (Figure 4). Mean CBV decreased by 17.8% and 20.6% in frontal regions, 23.0% and 25.1% in temporal regions, 22.0% and 22.2% in parieto-occipital regions, and 14.0% and 9.69% in posterior-fossa regions with right and left sided SCG stimulations respectively (all p-values < 0.01).

Although, both MTT and TMax increased with ipsilateral SCG stimulation, consistent with perfusion deficit, there was greater variability in the mean change (Figure 4). Mean MTT increased by 21.9% and 10.7% in frontal regions ($p=4.16\times10^{-3}$ and $p=1.03\times10^{-3}$), 21.6% and 13.0% in temporal regions ($p=0.010$ and $p=0.047$), and 21.7% and 15.7% in parieto-occipital regions ($p=2.09\times10^{4}$ and $p=2.24\times10^{-3}$) with right and left sided SCG stimulation respectively. While left SCG stimulation caused a 17.9% increase in MTT posterior-fossa regions that was statistically significant ($p=7.16\times10^{-3}$), right SCG stimulation caused a 15.6% increase in MTT that was approaching significance ($p=0.068$). Mean Tmax increased by 42.4% and 33.3% in frontal region, 59.1% and 46.7% in the temporal region, 46.3% and 38.2% in the parieto-occipital region, and 35.8% and 25.5% in posterior-fossa region with right and left sided SCG stimulation respectively (all p-values < 0.01).

Prior SCG blockade prevents cerebral hypoperfusion in setting of SCG stimulation

Prior lidocaine administration to the SCG inhibited the effects of SCG stimulation described above and restored cerebral perfusion. Mean CBF was less than 10% different from all measured regions compared to contralateral non-stimulated regions and this difference was not statistically significant compared to baseline (all $p>0.10$) (Figure 5). Similarly mean CBV was less than 5% different from all measured regions compared to contralateral non-stimulated regions and this difference was not statistically significant compared to baseline (all $p>0.10$).

Again, there was more variability with MTT and Tmax parameters when lidocaine was administered prior to SCG stimulation. Apart from the left frontal region, which had a mean 5.82% increase in MTT compared to the non-stimulated right frontal region ($p=0.0144$), and the right temporal region, which had a mean 4.13% decrease in MTT compared to the non-stimulated left temporal region ($p=8.06\times10^{-3}$), all other measured MTT means were within 15% of the non-stimulated contralateral side without statistical difference. For mean Tmax, measured values were within 20% of the non-stimulated contralateral side without statistical difference, except for the left frontal region that showed an 8.80% increase in mean Tmax compared to the non-stimulated right frontal region ($p=2.10\times10^{-3}$).

Discussion

To our knowledge, we are the first group to demonstrate true cerebral hypoperfusion from direct activation of the sympathetic nervous system in a large mammal. We used Yorkshire swine to develop a large mammal model of sympathetically-mediated cerebral hypoperfusion for translation into clinical application. Large mammals, such as the swine, more closely resemble human anatomy without the cost and other restrictions associated with canine and primate models. Additionally, swine cardiovascular anatomy is similar to that of humans and prior studies have used swine as experimental models to study cerebral vasospasm.[20–24]

An essential component to our model was the use of α-chloralose. α-chloralose is the preferred anesthetic for animal studies evaluating autonomic function as it provides depth of anesthesia, while maintaining high level of basal autonomic tone that is easily modified to produce robust responses.[22,25,26]

While the SCG is recognized to have sympathetic efferents, information regarding synaptic coverage, number of synapses and variability dependent on animal size and weight have not been well-characterized.[27] Hence, although we used ipsilateral mydriasis as a means to confirm sympathetic activation, we decided to stimulate the SCG at twice the current required to achieve mydriasis in order to ensure we elicited a robust activation of the SCG.

In addition to cerebral hypoperfusion, SCG stimulation induced a more striking perfusion deficit in extra-cranial regions evident on the CTp scans. This change was most evident in the snout, where there was blanching of the skin on the side of SCG stimulation. Although the carotid system in animals have greater proportional contribution to the external carotid distribution than seen in humans to supply the larger facial and masticatory muscles,

studies have shown anastomoses between external and internal carotid arteries in the swine that contribute to cerebral blood supply.[28–30] Therefore, we cautiously speculate that sympathetically-mediated hypoperfusion may have a greater effect on cerebral perfusion in humans than shown in our swine model, as the swine brain is more protected by significant extra-cranial collateral flow. Despite this added "protection," we were able to demonstrate significant cerebral perfusion deficits.

With respect to SCG blockade, we decided against using a longer-acting agent (i.e. Marcaine, acetylcholine receptor inhibitors), as doing so would increase the time required to recover to baseline and thereby unnecessarily lengthen the overall anesthesia time. In our study, we used a readily-available, short-acting sodium channel blocker, lidocaine. Although the exact duration of this effect was not measured, we found that we were able to re-demonstrate SCG-mediated ipsilateral perfusion deficit approximately 30 minutes after lidocaine administration (data not shown). Additionally, we did not see an increase in ipsilateral cerebral perfusion with lidocaine administration alone (in the absence of SCG stimulation) (data not shown). This suggests either low baseline sympathetic tone or a robust baseline brain perfusion that exceeds any hyper-perfusion attempts made with SCG inhibition alone.

The results of our work contribute to the current literature regarding sympathetic control in cerebral autoregulation. There have been controversial outcomes regarding the role of sympathetic nervous system in cerebral autoregulation. While some showed that resection of carotid sinus nerves in dog models abolished effect of cerebral autoregulation, others demonstrated that monkeys with chronic sympathetic denervation showed preserved cerebral autoregulation.[31,32] Controversial outcomes are also prevalent in human studies: Gierthmuhlen and colleagues demonstrated preserved cerebral autoregulation in patients with infarcted dorsolateral medulla oblongata (part of the sympathetic pathway)[33] but Zhang and colleagues showed significant changes to cerebral autoregulation response with sympathetic ganglion blockade.[34] Guo and colleagues suggest that such controversial results may be due to multiple compensatory mechanisms of cerebral autoregulation, heterogenous innervation of cerebral vasculature by the sympathetic nervous system and small samples size of prior studies.[35] Indeed, Gelpi and colleagues demonstrated that while cerebral autoregulation was preserved in subjects undergoing reflex sympathetic activation regardless of their history of recurrent postural syncope, those prone to postural syncope displayed more greater vagal withdrawal and less sympathetic activation associated orthostatic stressors.[36–40] Whereas the majority of prior studies have shown the effects of sympathetic blockade and/or denervation on cerebral autoregulation, our study provides a unique insight as we were able to stimulate the sympathetic nervous system to show a true cerebral perfusion deficit. Our results suggest that while other mechanisms of cerebral autoregulation may compensate for lack of sympathetic tone, overactivation of sympathetic nervous system at the level of SCG is sufficient to significantly alter cerebral blood flow in a swine model.

The role of parasympathetic activity in cerebral perfusion is still under investigation. While Yarnitsky et al have shown dilation of cerebral vessels with parasympathetic stimulation in a subarachnoid hemorrhage induced model of vasospasm in dogs, it is

unclear whether sympathetic hyperactivity or parasympathetic underactivity has a stronger influence on cerebral vasospasm.[41] Regardless, the ability to modulate both sympathetic and parasympathetic nervous systems remains a promising potential therapeutic intervention for cerebral ischemia associated with vasospasm, and deserves further investigation.

The main limitation to our study is perhaps, the simplification of using sympathetically-mediated hypoperfusion as a model for cerebral vasospasm. Recent studies show strong sympathetic activity in subarachnoid hemorrhage induced vasospasm in numerous animal models and suggest sympathetic modulation as a promising therapy.[19,21,42,43] We recognize that true cerebral vasospasm involves a complex interplay between various factors, but ultimately the clinically relevant end result of hypoperfusion is what we were able to achieve in our model.

Another limitation arises from the differences in swine and human cerebrovascular anatomy. Unlike in humans, swine common carotid artery bifurcates into the external carotid artery and the ascending pharyngeal artery, which later forms a rete mirabile before giving rise to internal cerebral arteries.[27,43] The rete mirabile, an arterial meshwork, is thought to have an evolutionary role in maintaining cerebral blood flow and blood temperature regulation in many mammalian species.[42,45] As such, the presence of carotid rete mirabile in swine may help guard against cerebral perfusion deficit. It is our belief that the observed perfusion deficit would have been even more pronounced without the protection of the rete mirabile and the extensive external to internal collaterals. While this is a limitation of the model, it may imply that the results are even more translatable to humans, who do not have such pronounced vascular protection mechanisms.

Intracranial pressure (ICP) can significantly affect the cerebral perfusion. Although it would have been interesting to measure ICP during our experiments, we did not do so for several reasons. Placing an ICP monitor introduces potential new variables, such as brain trauma, bleeding, or contamination of the intracranial space that may result in cerebral vasospasm and influence the outcomes of the SCG stimulation. Furthermore, ICP is arguably a global measure of the entire intracranial pressure and therefore significant changes in ICP would affect global cerebral perfusion. In this study, we stimulated the SCG one side at a time and observed differences in cerebral perfusion between the two hemispheres with a built-in contralateral control. We were unable to determine if SCG stimulation results in significant global ICP changes and if these changes affect the perfusion of the stimulated and/or non-stimulated side compared to baseline. Regardless, we believe our results are still quite valid given use of a contralateral built-in control.

Some have challenged the notion that vasospasm is the primary causative mechanism for delayed cerebral ischemia (DCI) following subarachnoid hemorrhage, endorsing spreading depolarization, microcirculatory dysfunction, disrupted cerebral autoregulation, and early brain injury as separate contributing factors.[46,47] While the exact pathophysiology of DCI in this setting remains unclear, resolution of vasospasm continues to be associated with good neurologic outcomes in patients following subarachnoid hemorrhage. Accordingly, reversal of cerebral vasospasm remains the standard of care and discovery of new methods

for reversing vasospasm continues to be an area of interest in the cerebrovascular research community.[48,49]

Conclusion

Our study demonstrates that sympathetic hyperactivity can lead to true cerebral hypoperfusion in a large mammal swine model. Furthermore, this activity can be inhibited with SCG blockade to restore cerebral perfusion. Accordingly, we propose further investigations into inhibition of SCG as a potential therapeutic option for cerebral hypoperfusion.

Acknowledgement:

Financial Disclosures:

1. Casa Colina Foundation research grant

Author: Geoffrey Colby MD PhD

Support: $50,000

2. NIH Research Education Programs (R25)

Author: Wi Jin Kim MD

Federal Identifier: NS079198

Organizational DUNS: 092530369

Support: $78,400

References

1. Armstead WM. Cerebral Blood Flow Autoregulation and Dysautoregulation. Anesthesiol Clin 2016: 465–477. [PubMed: 27521192]
2. Carter BS, Buckley D, Ferraro R, Rordorf G, Ogilvy CS. Factors associated with reintegration to normal living after subarachnoid hemorrhage. Neurosurgery 2000; 46: 1326–1333. [PubMed: 10834638]
3. Dorsch NWC, King MT. A review of cerebral vasospasm in aneurysmal subarachnoid haemorrhage Part I: Incidence and effects. J Clin Neurosci 1994; 1: 19–26. [PubMed: 18638721]
4. Proust F, Hannequin D, Langlois O, Freger P, Crissard P. Causes of morbidity and mortality after ruptured aneurysm surgery in a series of 230 patients: the importance of control angiography. Stroke 1995; 26: 1553–7. [PubMed: 7660397]
5. Naredi S, Lambert G, Eden E, All S, Runnerstam M, Rydenhag B, Friberg P. Increased sympathetic nervous activity in patients with nontraumatic subarachnoid hemorrhage. Stroke 2000; 4: 901–906.
6. Moussouttas M, Lai EW, Huyhn TT, James J, Strocks-Dietz C, Dombrowski K, Khoury J, Pacak K. Association between acute sympathetic response, early onset vasospasm, and delayed vasospasm following spontaneous subarachnoid hemorrhage. J Clin Neurosci 2014; 2: 256–262.
7. Takemoto Y, Hasegawa Y, Hayashi K, Cao C, Hamasaki T, Kawano T, Mukasa A, Kim-Mitsuyama S. The Stabilization of Central Sympathetic Nerve Activation by Renal Denervation Prevents Cerebral Vasospasm after Subarachnoid Hemorrhage in Rats. Transl Stroke Res 2019; doi: 10.1007/s12975-019-00740-9. [Epub ahead of print]
8. Lambert G, Naredi S, Eden E, Rydenhag B, Friberg P. Sympathetic nervous activation following subarachnoid hemorrhage: Influence of intravenous clonidine. Acta Anaesthesiol Scand 2002; 2: 160–165.

9. Hamel E Perivascular nerves and the regulation of cerebrovascular tone. J Appl Physiol 2006; 100: 1059–1064. [PubMed: 16467392]
10. Lee RH, Liu YQ, Chen PY, Liu CH, Chen MF, Lin HW, Kuo JS, Premkumar LS, Lee TJ. Sympathetic α3β2-nAChRs mediate cerebral neurogenic nitrergic vasodilation in the swine. Am J Physiol Heart Circ Physiol 2011; 301: H344–H354. [PubMed: 21536845]
11. Lee TJ, Chang HH, Lee HC, Chen PY, Lee YC, Kuo JS, Chen MF. Axo-axonal interaction in autonomic regulation of the cerebral circulation. Acta Physiol (Oxf) 2011; 203: 25–35. [PubMed: 21159131]
12. Wu CY, Lee RH, Chen PY, Tsai AP, Chen MF, Kuo JS, Lee TJ. L-type calcium channels in sympathetic $\alpha_3\beta_2$-nAChR-mediated cerebral nitrergic neurogenic vasodilation. Acta Physiol (Oxf) 2014; 211: 544–558. [PubMed: 24825168]
13. Tuor UI. Local distribution of the effects of sympathetic stimulation on cerebral blood flow in the rat. Brain Res 1990; 529: 224–231. [PubMed: 2282493]
14. Kurth CD, Wagerle LC, Delivoria-Papadopoulos M. Sympathetic regulation of cerebral blood flow during seizures in newborn lambs. Am J Physiol 1988; 255: H563–H568. [PubMed: 3137827]
15. Edvinsson L Neurogenic mechanisms in the cerebrovascular bed: autonomic nerves, amine receptors and their effects on cerebral blood flow. Acta Physiol Scand Suppl 1975; 427: 1–35. [PubMed: 56123]
16. Dagistan Y, Kilinc E, Balci CN. Cervical sympathectomy modulates the neurogenic inflammatory neuropeptides following experimental subarachnoid hemorrhage in rats. Brain Res 2019; 1722
17. Lee RH, Couto e Silva A, Lerner FM, Wilkins CS, Valido SE, Klein DD, et al. Interruption of perivascular sympathetic nerves of cerebral arteries offers neuroprotection against ischemia. Am J Physiol Heart Circ Physiol 2016; 312: H182–H188. [PubMed: 27864234]
18. Treggiari MM, Romand JA, Martin JB, Reverdin A, Rufenacht DA, Tribolet Nd. Cervical Sympathetic Block to Reverse Delayed Ischemic Neurological Deficits After Aneurysmal Subarachnoid Hemorrhage. Stroke 2003; 34: 961–967.
19. Beam DM, Neto-Neves EM, Stubblefield WB, Alves NJ, Tune JD, Kline JA. Comparison of isoflurane and alpha-chloralose in an anesthetized swine model of acute pulmonary embolism producing right ventricular dysfunction. Comp Med 2015; 65: 54–61. [PubMed: 25730758]
20. Zibly Z, Fein L, Sharma M, Assaf Y, Wohl A, Harnof S. A novel swine model for subarachnoid hemorrhage-induced vasospasm. Neurology India 2017; 65(5): 1035–42. [PubMed: 28879893]
21. Byrne JV, Griffith TM, Edwards DH, Harrison TJ, Johnston KR. Investigation of the vasoconstrictor action of subarachnoid haemoglobin in the pig cerebral circulation *in vivo*. Br J Pharmacol 1989;97:669–74. [PubMed: 2788022]
22. Ebel H, Semmelmann G, Friese M, Volz M, Lee JY, Duck M, et al. Effects of electrical stimulation of the Gasserian ganglion on regional cerebral blood flow after induced subarachnoid hemorrhage in pigs evaluated by 99mTc-HMPAO-SPECT. Minim Invasive Neurosurg 2001;44:50–7. [PubMed: 11409313]
23. Salar G, Ori C, Iob I, Costella GB, Battaggia C, Peserico L. Cerebral blood flow changes induced by electrical stimulation of the Gasserian ganglion after experimentally induced subarachnoid haemorrhage in pigs. Acta Neurochir 1992;119:115–20. [PubMed: 1481737]
24. Mangla S, Choi JH, Barone FC, Novotney C, Libien J, Lin E, Pile-Spellman J. Endovascular external carotid artery occlusion for brain selective targeting: a cerebrovascular swine model. BMC Res Notes 2015; 8: 808. [PubMed: 26689288]
25. Yoneda I, Nishizawa M, Benson KT, Chaffee TL, Goto H. Attenuation of arterial baroreflex control of renal sympathetic nerve activity during lidocaine infusion in alpha-chloralose-anesthetized dogs. Acta Anaesthesiol Scand 1994; 38(1): 70–4. [PubMed: 8140878]
26. Mori T, Nishikawa K, Terai T, Yukioka H, Asada A. The effects of epidural morphine on cardiac and renal sympathetic nerve activity in alpha-chloralose-anesthetized cats. Anesthesiology 1998; 88(6): 1558–65. [PubMed: 9637650]
27. Lobo Ladd FV, Lobo Ladd AAB, da Silva AAP, Augusto Coppi A. Stereological and Allometric Studies on Neurons and Axo-Dendritic Synapses in Superior Cervical Ganglia. Int Rev Cell Mol Biol 2014; 311: 123–155. [PubMed: 24952916]

28. Meadow W, Rudinsky B, Raju T, John E, Fornell L, Shankararao R. Correlation of flow probe determinations of common carotid artery blood flow and internal carotid artery blood flow with microsphere determinations of cerebral blood flow in piglets. Pediatr Res 1999; 45: 324–30. [PubMed: 10088649]
29. Daniel PM, Dawes JKD, Pichard MML. Studies on the carotid rete and its associated arteries. Phil Trans R Soc Land B 1953; 237: 173–208.
30. Weenink RP, Hollmann MW, Stevens MF, et al. Cerebral arterial gas embolism in swine. Comparison of two sites for air injection. J Neurosci Methods 2011; 194(2): 336–341. [PubMed: 21074559]
31. Sagawa K, Guyton AC. Pressure-flow relationships in isolated canine cerebral circulation. Am J Physiol 1961; 200: 711–4. [PubMed: 13745365]
32. Eklof B, Ingvar DH, Kagstrom E, Olin T. Persistence of cerebral blood flow autoregulation following chronic bilateral cervical sympathectomy in the monkey. Acta Physiol Scand 1971; 82(2): 172–176. [PubMed: 4997250]
33. Gierthmuhlen J, Allardt A, Sawade M, Baron R, Wasner G. Dynamic cerebral autoregulation in stroke patients with a central sympathetic deficit. Acta Neurol Scand 2011; 123(5): 332–338. [PubMed: 20809903]
34. Zhang R, Zuckerman JH, Iwasaki K, Wilson TE, Crandall CG, Levine BD. Autonomic neural control of dynamic cerebral autoregulation in humans. Circulation 2002; 106(14): 1814–1820 [PubMed: 12356635]
35. Guo ZN, Shao A, Tong LS, Sun W, Liu J, Yang Y. The Role of Nitric Oxide and Sympathetic Control in Cerebral Autoregulation in the Setting of Subarachnoid Hemorrhage and Traumatic Brain Injury. Mol Neurobiol 2016; 53(6): 3606–3615. [PubMed: 26108186]
36. Gelpi F, Bari V, Cairo B, et al. Dynamic cerebrovascular autoregulation in patients prone to postural syncope: comparison of techniques assessing the autoregulation index from spontaneous variability series. Auton Neurosci 2022; 237: 102920. [PubMed: 34808528]
37. Marchi A, Bari V, Maria BD, et al. Calibrated variability of muscle sympathetic nerve activity during graded head-up tilt in humans and its link with noradrenaline data and cardiovascular rhythms. Am J Physiol Regul Integr Comp Physiol 2016; 310(11): R1134–43. [PubMed: 27009053]
38. Furlan R, Porta A, Costa F, et al. Oscillatory patterns in sympathetic neural discharge and cardiovascular variables during orthostatic stimulus. Circulation 2000; 101(8): 886–92. [PubMed: 10694528]
39. Cooke WH, Hoag JB, Crossman AA, Kuusela TA, Tahvanainen KU, Eckberg DL. Human responses to upright tilt: a window on central autonomic integration. J Physiol 1999; 517: 617–28. [PubMed: 10332107]
40. Montano N, Ruscone TG, Porta A, Lombardi F, Pagani M, Malliani A. Power spectrum analysis of heart rate variability to assess changes in sympatho-vagal balance during graded orthostatic tilt. Circulation 1994; 90(4): 1826–31. [PubMed: 7923668]
41. Yarnitsky D, Lorian A, Shalev A, et al. Reversal of cerebral vasospasm by sphenopalatine ganglion stimulation in a dog model of subarachnoid hemorrhage. Surg Neurol 2005; 64(1): 5–11. [PubMed: 15993169]
42. Goellner E, Slavin KV. Cervical spinal cord stimulation may prevent cerebral vasospasm by modulating sympathetic activity of the superior cervical ganglion at lower cervical spinal level. Med Hypotheses 2009; 73(3): 410–3. [PubMed: 19409714]
43. Chun-jing H, Shan O, Guo-dong L, Hao-xiong N, Yi-ran L, Ya-ping F. Effect of cervical sympathetic block on cerebral vasospasm after subarachnoid hemorrhage in rabbits. Acta Cir Bras 2013; 28(2): 89–93. [PubMed: 23370920]
44. Ashwini CA, Shubha R, Jayanthi KS. Comparative anatomy of the circle of Willis in man, cow, sheep, goat, and pig. Neuroanatomy 2008; 7: 54–65.
45. Barnett C, Marsden C. Functions of the Mammalian Carotid Rete Mirabile. Nature 1961; 191: 88–89. [PubMed: 13687125]

46. Dodd WS, Laurent D, Dumont AS, et al. Pathophysiology of Delayed Cerebral Ischemia after Subarachnoid Hemorrhage: A Review. J Am Heart Assoc 2021; 10(15):e021845. [PubMed: 34325514]

47. Dankbaar JW, Rijsdijk M, van der Schaaf IC, Velthuis BK, Wermer MJH, Rinkel GJE. Relationship between vasospasm, cerebral perfusion and delayed cerebral ischemia after aneurysmal subarachnoid hemorrhage. Neuroradiology 2009; 51(12): 813–819. [PubMed: 19623472]

48. Mao G, Gigliotti MJ, Esplin N, Sexton K. The clinical impact and safety profile of high-dose intra-arterial verapamil treatment for cerebral vasospasm following aneurysmal subarachnoid hemorrhage. Clin Neurol Neurosurg 2021; 202: 106546. [PubMed: 33588359]

49. Djilvesi D, Horvat I, Jelaca B, Golubovic J, Pajicic F, Vulekovic P. Comparison of radiological versus clinical cerebral vasospasm after aneurysmal subarachnoid hemorrhage: is vasospasm always present? Neurol Res 2020: 42(12): 1027–1033. [PubMed: 32893749]

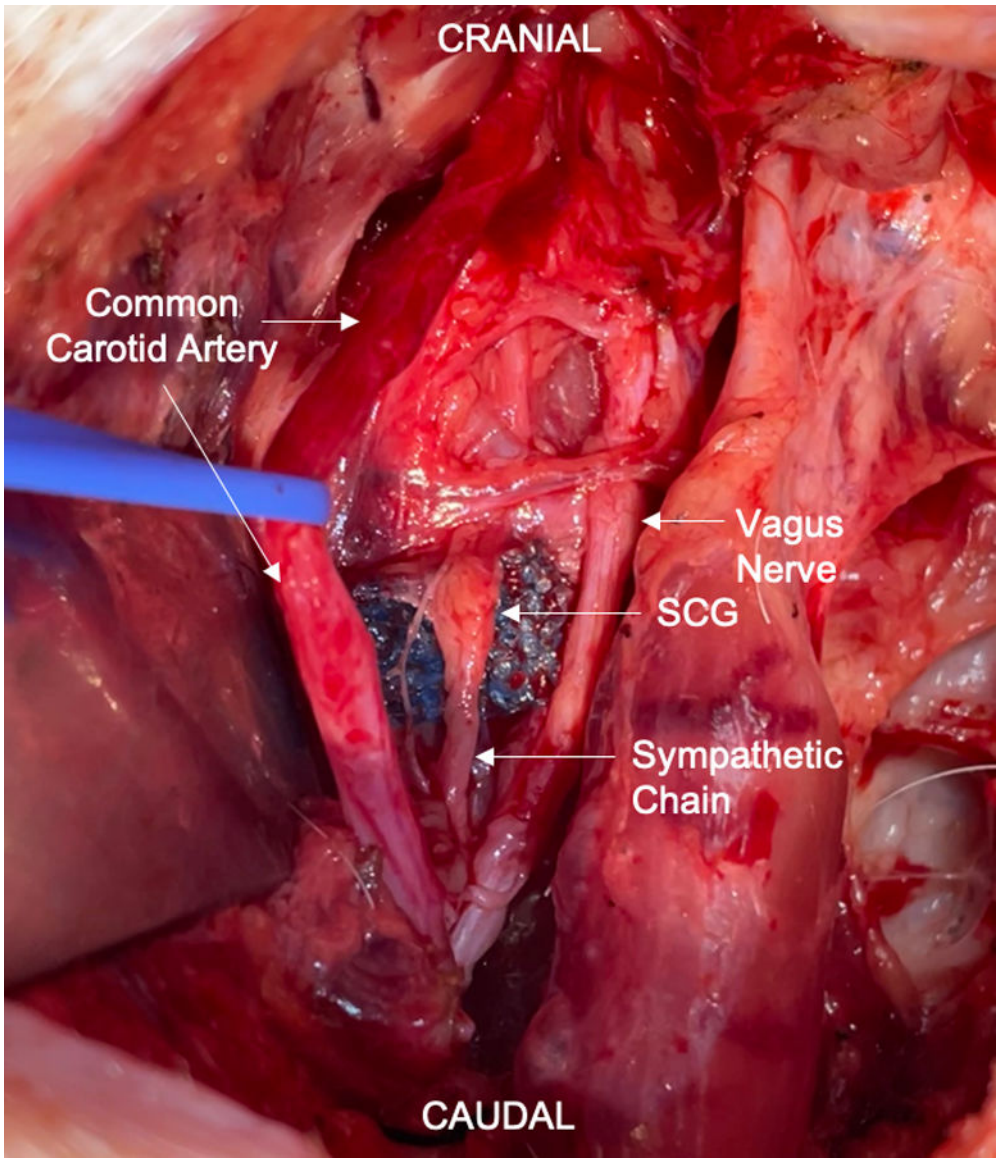

Figure 1:

Swine left neck dissection photograph

After proper intubation and sedation of the animal a vertical incision was made in the ventral left side of the animal's neck to expose the SCG.

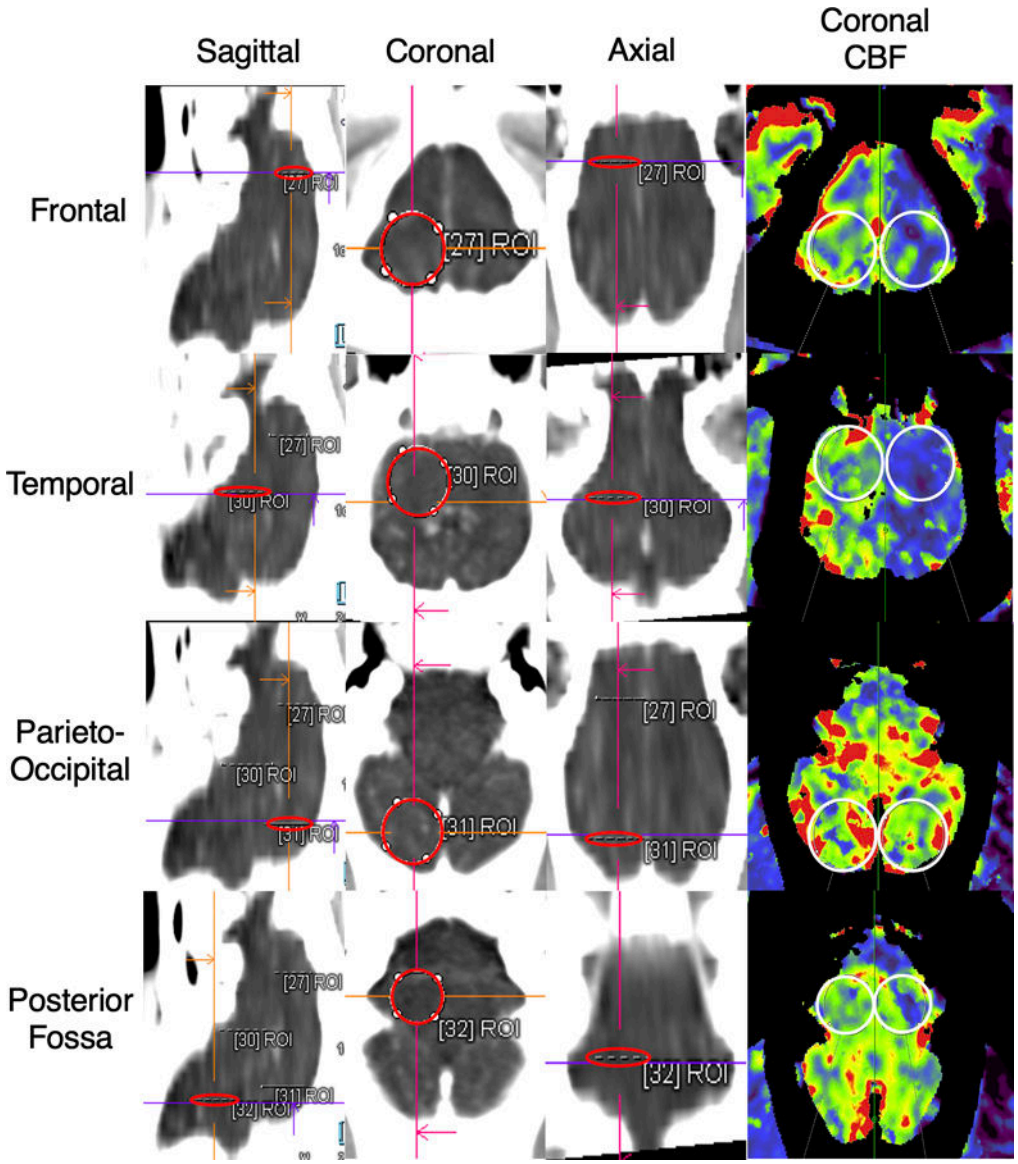

Figure 2:

Representative Regions of Interest

Examples of representative regions of interest (ROI) in Frontal, Temporal, Parieto-Occipital and Posterior Fossa regions. Red circles show representative ROIs on sagittal, coronal and axial views of the right hemisphere. White circles show applied ROIs on processed coronal cerebral blood flow (CBF) imaging. Right sided ROI was auto-mirrored to left hemisphere for comparison.

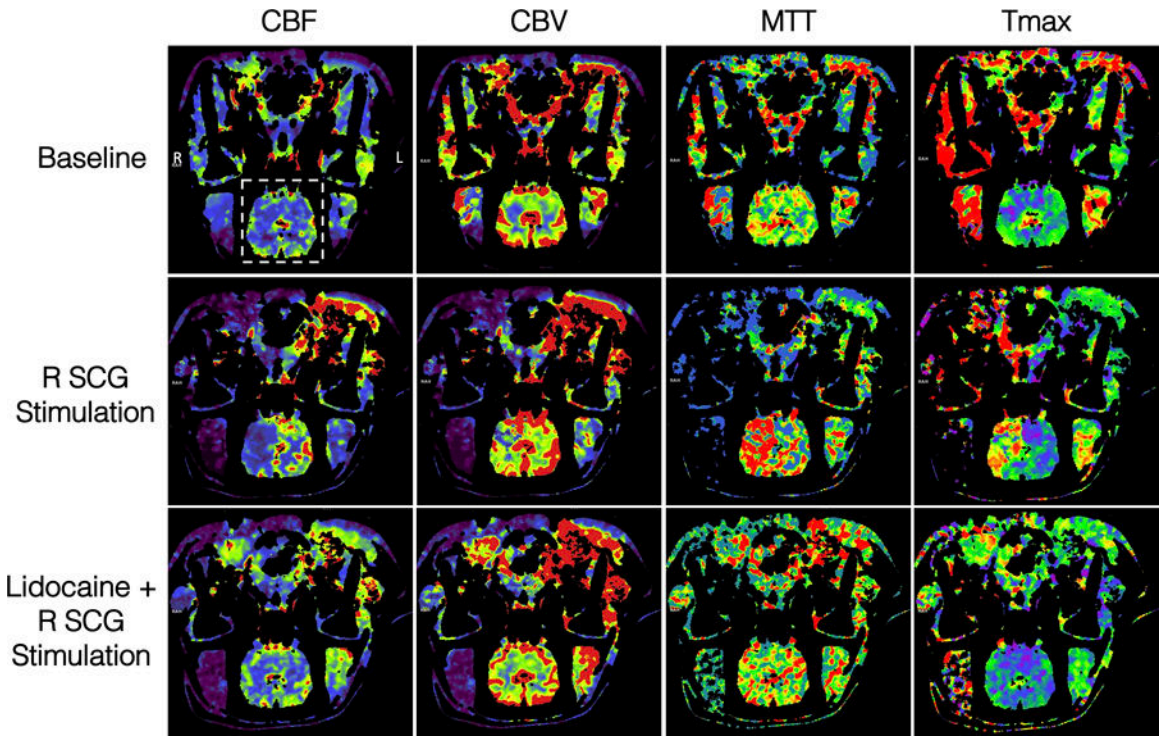

Figure 3:

Computed Tomography Perfusion Scans

CTp coronal view in standard radiographic orientation of fronto-temporal area of swine brain. White dashed box shows the location of swine brain. Cerebral blood flow (CBF), cerebral blood volume (CBV), mean transit time (MTT) and time-to-maximum (Tmax) shown in different columns. CTp of swine at baseline, with stimulation of right SCG with and without prior lidocaine administration shown in different rows.

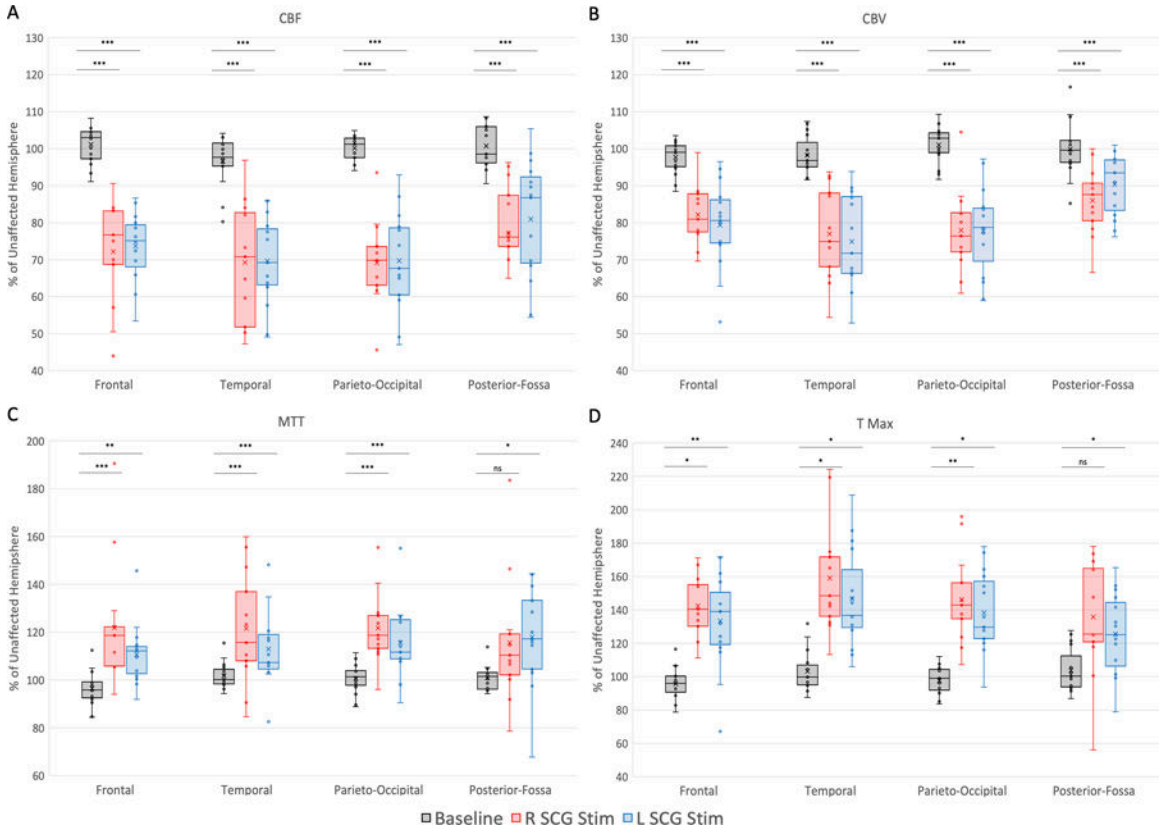

Figure 4:

CTp parameters in intracranial areas

Measurements ipsilateral to side SCG stimulation represented as a percentage of non-stimulated contralateral side. Baseline (no SCG stimulation) shows right cerebral blood flow as a percentage of L side. (A) Cerebral blood flow (CBF); (B) Cerebral blood volume (CBV); (C) Mean transit time (MTT); (D) time-to-maximum. Box indicates first to third quartile of data points. Whiskers indicate data set range within 1.5 times interquartile range from the box. Line within box indicates median. “X” within box indicates mean. Black: baseline (no SCG stimulation); Red (solid): right SCG stimulation; Blue (solid): left SCG stimulation; (*: $p < 0.05$; **: $p < 0.001$; ***: $p < 0.0001$)

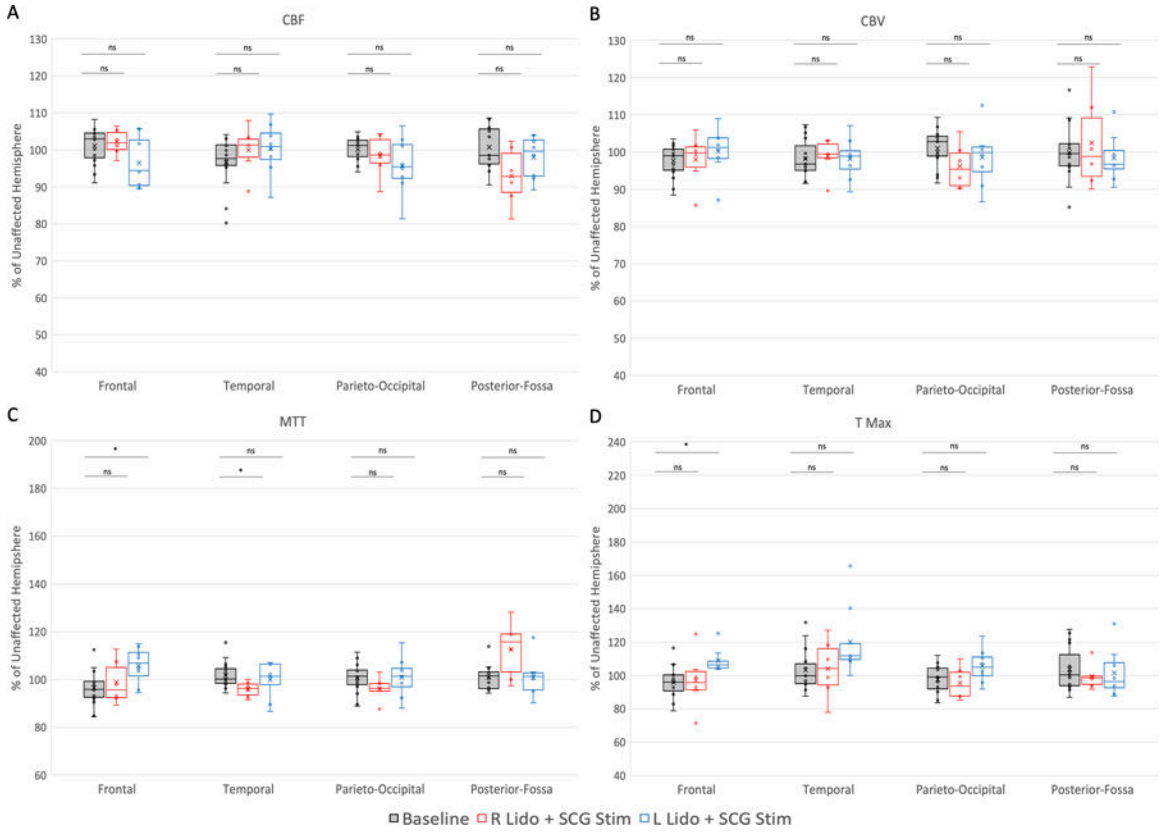

Figure 5:

CTp parameters with SCG blockade in intracranial areas

Measurements ipsilateral to side of SCG stimulation represented as a percentage of non-stimulated contralateral side. Baseline (no SCG stimulation) shows right cerebral blood flow as percentage of left side. (A) Cerebral blood flow (CBF); (B) Cerebral blood volume (CBV); (C) Mean transit time (MTT); (D) time-to-maximum. Box indicates first to third quartile of data points. Whiskers indicate data set range within 1.5 times interquartile range from the box. Line within box indicates median. “X” within box indicates mean. Black: baseline (no SCG stimulation); Red (empty): right SCG stimulation with 2% lidocaine administration; Blue (empty): left SCG stimulation with 2% lidocaine administration. (*: $p < 0.05$; ns: non-significant)